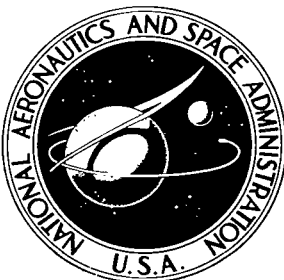


NASA TECHNICAL NOTE



NASA TN D-5247

C. 1

NASA TN D-5247

032034



TECH LIBRARY KAFB, NM

LOAN COPY: RETURN TO
AFWL (WLIL-2)
KIRTLAND AFB, N MEX

LEED STUDY OF THE ADHESION OF VARIOUS MATERIALS TO THE (111) SURFACE OF NICKEL

by Donald H. Buckley
*Lewis Research Center
Cleveland, Ohio*

TECH LIBRARY KAFB, NM



0132034

LEED STUDY OF THE ADHESION OF VARIOUS MATERIALS TO
THE (111) SURFACE OF NICKEL

By Donald H. Buckley

Lewis Research Center
Cleveland, Ohio

NATIONAL AERONAUTICS AND SPACE ADMINISTRATION

For sale by the Clearinghouse for Federal Scientific and Technical Information
Springfield, Virginia 22151 - CFSTI price \$3.00

ABSTRACT

Adhesion studies were made with copper, tungsten, oxidized tungsten, and quartz contacting a nickel (111) surface. The copper, tungsten, oxidized tungsten, and quartz were in the form of 1 mm diameter flat ended fibers. Loads of 20 to 150 mg were employed with surface contact times of 10 to 300 sec. The nickel (111) surface was examined before and after adhesion contact with LEED. With clean metals, fracture in tension occurred in the lower cohesive strength material. When copper contacted nickel, a surface alloy formed. The contacting of clean nickel with an oxidized tungsten surface resulted in oxygen transfer from tungsten to nickel with surface rearrangement. Quartz adhered to nickel with fracture occurring in the quartz on separation of the surfaces.

LEED STUDY OF THE ADHESION OF VARIOUS MATERIALS TO THE (111) SURFACE OF NICKEL

by Donald H. Buckley

Lewis Research Center

SUMMARY

An investigation was conducted to determine the nature of adhesion of four materials to a nickel (111) surface using LEED. The four materials contacting the nickel (111) surface were copper, tungsten, oxidized tungsten, and quartz. These four materials were in the form of 1-millimeter-diameter flat ended fibers. Adhesion contact was made at loads from 20 to 150 milligrams and at contact times from 10 to 300 seconds.

The results of the investigation indicate that, with clean metal surfaces in contact, fracture in tension of adhesive contacts occurs in the lower cohesive strength material; that is, cohesive rather than adhesive bonds are broken. With copper, an alloy was observed to form on the nickel surface. Contacting clean nickel with oxidized tungsten resulted in oxygen transfer to nickel by tungsten oxide reduction and subsequent surface rearrangement of the oxygen on nickel. With quartz, adhesion of the quartz to nickel occurred with fracture taking place in the quartz on separation of the surfaces.

INTRODUCTION

There are a number of devices which have been used in recent years to aid in the study of the atomic nature of solid surfaces. One device which appears especially useful in the study of adhesion is LEED (low-energy electron diffraction). With LEED, it should be possible to determine surface changes which occur in the outermost atomic layers as a result of the contact of two solid surfaces.

The metal which has probably been examined with LEED in more detail than any other, with the exception of tungsten, is nickel. Various atomic planes of nickel have been examined in the clean state and in the presence of various adsorbed surface films (refs. 1 to 10). From a practical point of view, it is a metal of extreme interest in the

field of catalysis and should be of interest to the field of lubrication because of its use in alloy form in this field.

The objective of this investigation was to examine, with LEED, the adhesion of three materials in contact with the (111) close-packed plane of nickel. The (111) plane of nickel was selected for study for the following reasons: (1) it has the highest modulus of elasticity, and therefore, the greatest resistance to plastic deformation, (2) it has the least chemically active surface (ref. 11), and (3) in adhesion studies with another face-centered cubic metal, copper, this particular plane exhibits the least tendency toward adhesion (ref. 12).

The materials examined in contact with the (111) nickel surface were (1) copper, (2) tungsten, (3) oxidized tungsten, and (4) quartz. Copper was selected because it is not as strong as nickel; hence, it was anticipated fracture would occur in copper on the breaking of junctions. Tungsten was examined for the opposite reason, namely, that with tungsten in contact with nickel, adhesion of nickel to tungsten would occur. Oxidized tungsten was studied in contact with nickel to determine if oxygen "uptake" would occur. Lastly, quartz was examined because it is noncrystalline in the form used and a source of oxygen from a brittle material. Further, it should not superimpose a pattern on nickel.

Experiments were conducted with 1-millimeter-diameter flats of the above mentioned materials in contact with the nickel (111) face at loads from 20 to 150 milligrams and contact times from 10 to 300 seconds. All experiments were conducted in a vacuum of 8.0×10^{-11} to 2.0×10^{-10} torr.

MATERIALS

The nickel used in this study was triple-zone vacuum refined, containing as the principal bulk impurities 37 ppm carbon, 18 ppm oxygen, 3 ppm nitrogen, and 12 ppm iron. The fiber materials, copper and tungsten, were also of high purity as was the quartz. The oxygen and hydrogen gases were of a reagent grade. Mass spectrometer analysis of the hydrogen (high purity) indicated the presence of hydrocarbons. The gas was therefore purified before use by passing it through liquid-nitrogen-cooled molecular sieve material.

EXPERIMENTAL PROCEDURE

The nickel crystals used in this study were electric discharge machined from a rod into specimens 6 millimeters in diameter by 3 millimeters thick. They were polished on abrasive paper down to 600 grit and then electropolished in phosphoric acid to remove the worked layer. Orientation was determined initially before and rechecked after

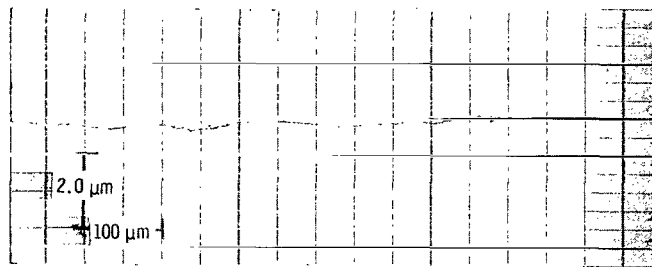


Figure 1. - Surface profile of electropolished (111) nickel surface.

machining by the Laue X-ray technique. The crystals were spot welded (on the flat face opposite that used in the experiments) to a tantalum holder for resistance heating. They were then mounted in the apparatus.

A surface profile of the nickel surface obtained with a surface profilometer is shown in figure 1. It is of interest to note that the characteristic asperities frequently shown for surfaces in lubrication studies are not present. It appears as if these are removed in the electropolishing process or are of such small size as to be unresolved at the magnifications indicated.

APPARATUS

The apparatus used in these studies is shown schematically in figure 2. The single-crystal surface mounted in the center of the chamber could be rotated 360° . This rotatability allowed for the making of adhesion measurements on the crystal surface shown in

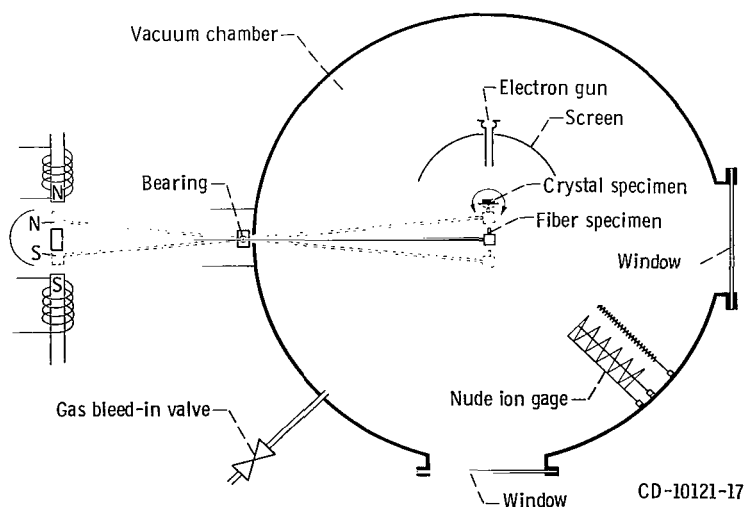


Figure 2. - LEED adhesion apparatus.

figure 1, then rotating the crystal 180° and obtaining a LEED pattern from the crystal surface in the adhesion contact area. The crystal could also be moved in the lateral and vertical directions.

The crystal specimen was supported in the chamber by means of two insulated metal rods, and a thin tantalum holder was used to resistance heat the crystal. A 100 ampere ac power supply was used for resistance heating.

The fiber, which contacted the single-crystal metal surface, was mounted in a stainless-steel holder which was, in turn, mounted to a 1.5-millimeter-diameter stainless-steel beam. The beam was mounted in a bearing containing yoke. At the end of the beam beyond the pivot point, and opposite the fiber specimen, was a small permanent magnet. Outside the chamber wall were two electromagnets. The permanent and electromagnets were positioned in such a manner as to have like poles facing each other. A simple variation in the current applied to the magnets could be used to move the beam.

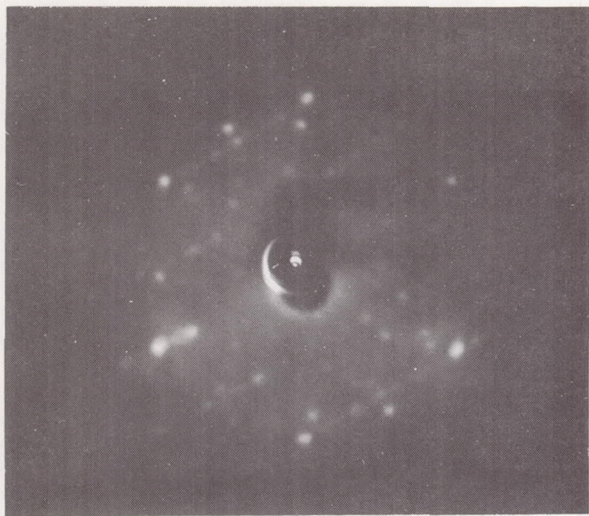
The current applied to the electromagnets was calibrated in terms of the force applied in the adhesion experiments. Load applied to the surfaces in contact was measured by current as was the force required to separate the crystal surfaces.

The LEED electron optics and the vacuum system were of the standard type used by those engaged in LEED studies and is adequately described in the literature (refs. 13 and 14). The basic LEED system was obtained commercially. The electron optics system was of the Varian three-grid type. The diameter of the beam was 0.6 millimeter. The vacuum system consisted of vacsorb pumps, an ion pump, and a sublimation pump. The system pressure was measured with a nude ion gage and all experiments were conducted with the vacuum system in the range of pressures from 8.0×10^{-11} to 2.0×10^{-10} torr. No cryopumping was used.

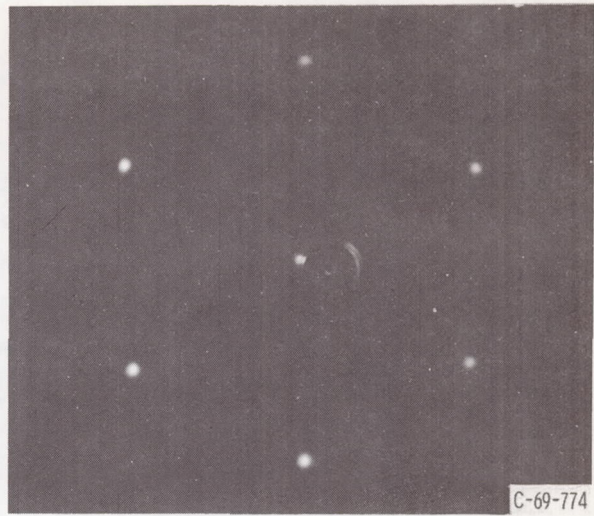
RESULTS AND DISCUSSION

The (111) nickel surface, as it relates to the other atoms within the framework of the face-centered cubic structure, is shown in figure 3 at the top. The ABC layer stacking is shown with the (111), or A, surfaces indicated. The A surface shown in the plan view is reproduced in the lower part of figure 2 indicating the unit mesh.

If the nickel surface is heated for 3 hours to 1000° C in vacuum, the LEED pattern obtained is that shown in figure 4(a). The nickel is covered with a structure resulting from the diffusion of carbon to the nickel surface on heating. The methods for cleaning such a nickel surface are described in the literature (refs. 8 and 10). It consisted essentially of reacting the surface with oxygen to remove carbon and subsequent oxygen removal with hydrogen and, finally, heating to remove hydrogen. The pattern of figure 4(b) was obtained after this process for the clean nickel surface. The structure of figure 4(b) relates as it should to the atomic arrangement of the surface indicated in figure 3.



(a) Single heating of crystal in vacuum to 1000° C; contaminated surface; 110 volts.



(b) Hydrogen cleaning of surface subsequent heating to 1000° C; clean surface; 75 volts. C-69-774

Figure 4. - Photographs of nickel (111) surface contaminated and hydrogen cleaned.

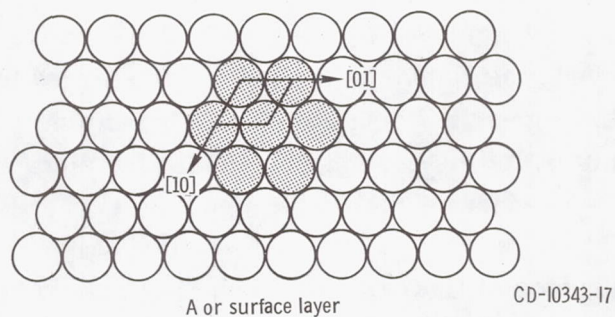
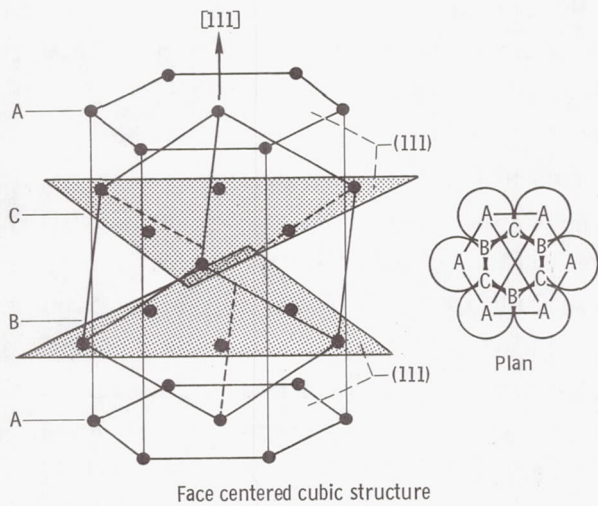


Figure 3. - (111) Atomic arrangement and surface structure with unit mesh for face-centered cubic system (e.g., nickel).

ADHESION WITH COPPER

Adhesion experiments were made with copper contacting the (111) nickel surface under a load of 20 milligrams for a contact time of 10 seconds. When the specimens were separated (separation requiring a force of 80 mg), the pattern of figure 5(a) was obtained. The pattern of figure 5(a) is for clean copper in contact with the nickel surface. If the copper were not clean, this pattern was not obtained.

The pattern of figure 5(a) represents the uptake of copper into the nickel surface structure in an ordered fashion as shown with the aid of figure 6. Copper at these light loads is not transferred to the nickel surface in random spots where adhesion of the copper occurred but rather in a very definite lattice site. The LEED pattern would indicate the formation of a surface alloy of copper in nickel with an alloy-type structure.

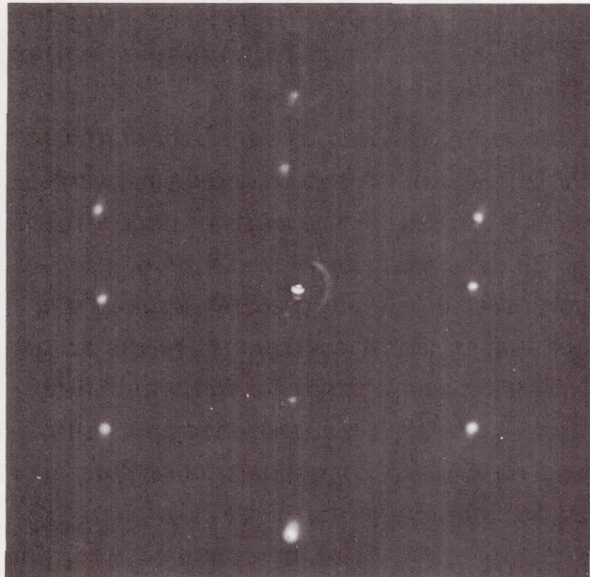
The nickel lattice has been expanded in figure 5(a) with the addition of copper in keeping with Vegard's Law for solid solutions in the bulk. Nickel has a lattice parameter of 3.5238 Å, a distance of closest approach of 2.491 Å, and an atomic radius of 1.24 Å. Copper has a lattice parameter of 3.6153 Å, a distance of closest approach of 2.556 Å, and an atomic radius of 1.28 Å. The deviation from Vegard's Law is slight and the nickel lattice normally in the bulk continues to expand on the addition of copper. Since the atomic arrangement for a clean nickel surface is the same as is the bulk (i.e., the surface plane of atoms is parallel to planes in the bulk (ref. 13)), alloying behavior would not be expected to differ markedly, thus explaining the expansion of figure 5(a).

The formation of surface alloys has been observed with vapor deposition of gold on a clean copper (100) surface at room temperature (ref. 15). With vapor deposition, the metal atoms arrive at the surface in the vapor phase and must, although the authors of reference 15 did not so specifically state, rearrange after surface arrival. In the study reported herein, however, the copper contacts the nickel in the solid state, adhesion of copper to nickel occurs and copper rearrangement must subsequently take place.

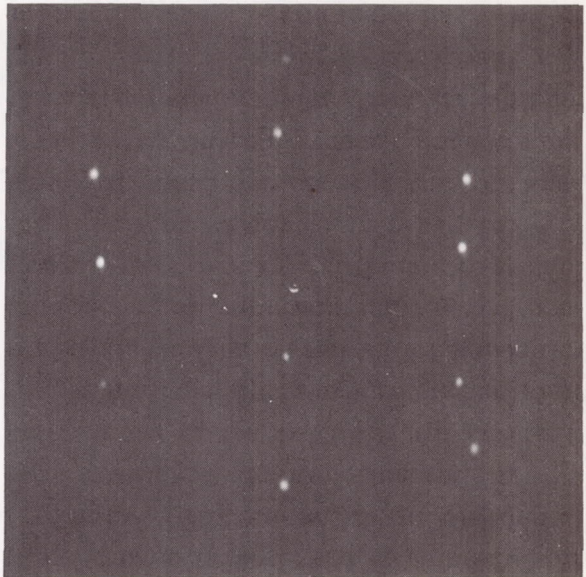
The ordering of copper in the nickel as seen in figure 5(a) is not seen in bulk alloying (refs. 16 and 17). In reference 16, care was taken, however, not to preclude its existence. Such observations of surface behavior warn against the use of bulk properties in a consideration of surface phenomena such as adhesion.

The LEED patterns of figures 5(a), (b), and (c) at various loads indicate that, within the load range employed, the copper is not being transferred to the nickel by subsurface fracture but rather the copper is being atomically transferred from the surface. It must be pointed out that this is not the case at heavier loads; also, even at light loads, the possibility of bulk transfer cannot be excluded. Under heavy loads, fracture in the copper bulk will occur.

In the light load region of figure 5 then, one would not apply fracture mechanics to the adhesion process but rather one would apply cohesive energy considerations. Since



(a) 20 milligrams; 75 volts.



(b) 80 milligrams; 75 volts.



C-69-775

(c) 150 milligrams; 75 volts.

Figure 5. - Photographs of nickel (111) surface after contact of that surface with 1-millimeter-diameter copper fiber.

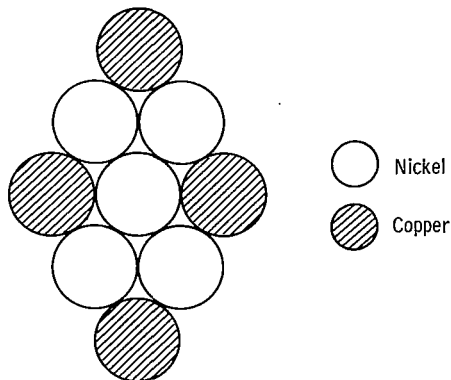


Figure 6. - Atomic arrangement of copper in nickel lattice.

the transfer process occurs by an adhesion of copper atoms to nickel, there must be a breaking of cohesive bonds in the copper. This, of course, means that the cohesive copper-to-copper bonds are weaker than the copper-to-nickel adhesive bonds. This is not surprising since many compounds and alloys are stronger than either of the parent materials (ref. 18).

Since cohesive energy in copper is that which must be overcome in separating the surfaces of copper and nickel, then it is worthwhile to examine briefly the concept of cohesive strength. It could be approached from a chemical bonding point of view, but this would be a laborious process, and the results might not be too reliable. A better and simpler approach is to compare physical properties with cohesive strength.

There are four very simple equations which have been developed for cohesive strengths and these are discussed in reference 18. The simplest is

$$C_s = 0.52 \left(\frac{E\tau}{y_0} \right)^{1/2}$$

where

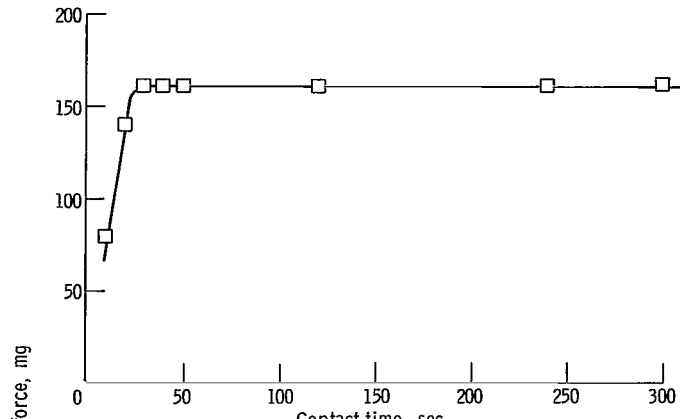
C_s cohesive stress, dynes/cm²

E Young's modulus, dynes/cm²

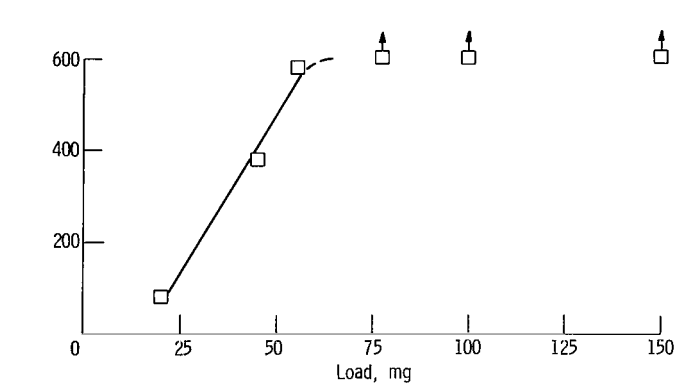
τ surface energy, dynes/cm²

y_0 initial atomic separation

The first observation for cohesive energy is that if adhesion occurs with stronger bonding than in either of the parent materials, copper will adhere to nickel. This is what has been observed (fig. 5). Using this equation a cohesive energy of 2.0×10^{11} dynes per square centimeter is obtained. This then would be the force required to separate the specimen if



(a) Contact time. Load applied, 20 milligrams.



(b) Load. Contact time, 10 seconds.

Figure 7. - Force of adhesion of copper to nickel (111) as function of contact time and load. Copper diameter 1.0 millimeter; temperature, 20° C; ambient pressure, 1.0×10^{-10} torr.

it were not for crystal imperfections. If the real contact area were known, by resistivity or some other measurement, the actual forces of adhesion in figure 7 could be compared directly to the cohesive strength of the copper to determine the effect of imperfections.

If contact area is calculated from the applied load in the experiment and the tensile cohesive strength of the copper is calculated from contact area, a value of 2.5×10^8 dynes per square centimeter is obtained. This value is nearly three orders of magnitude lower than the calculated cohesive strength of copper of 2.0×10^{11} dynes per square centimeter. The large difference may be due to vacancies and dislocations in the copper and misfit dislocations at the copper-nickel interface.

The effect of contact time and load on the force required to separate a copper-nickel adhesion couple is shown in figure 7. The initial dependence of the adhesion force on contact time in figure 7(a) is indicative of plastic behavior of the copper even at the very light

load employed. Localized creep occurs until the load is supported (in fig. 7(a), up to a contact time of 30 sec) and then the adhesion force is independent of contact time (30 to 300 sec contact time in fig. 7(a)).

The adhesive force for copper to nickel is presented at various loads in figure 7(b). Each data point represents an average of six data points obtained at different locations on the crystal face. The force of adhesion at a load of 20 milligrams and 10-second contact time was approximately four times the applied load. At applied loads of 40 and 60 milligrams the force required to separate the surfaces was approximately 10 times that of the applied load. With loads in excess of 60 milligrams, the adhesion force was in excess of 600 milligrams and beyond the measurement limits of the apparatus. The separation force at light loads is a function of the contact area and the cohesive strength of the copper, the area increasing with increase in load or applied stress.

ADHESION WITH TUNGSTEN

If the fiber specimen contacting the nickel (111) had a markedly higher strength than nickel (rather than lower, as for copper), it would be anticipated that the changes discussed in reference to copper earlier would now take place in the nickel surface being ex-

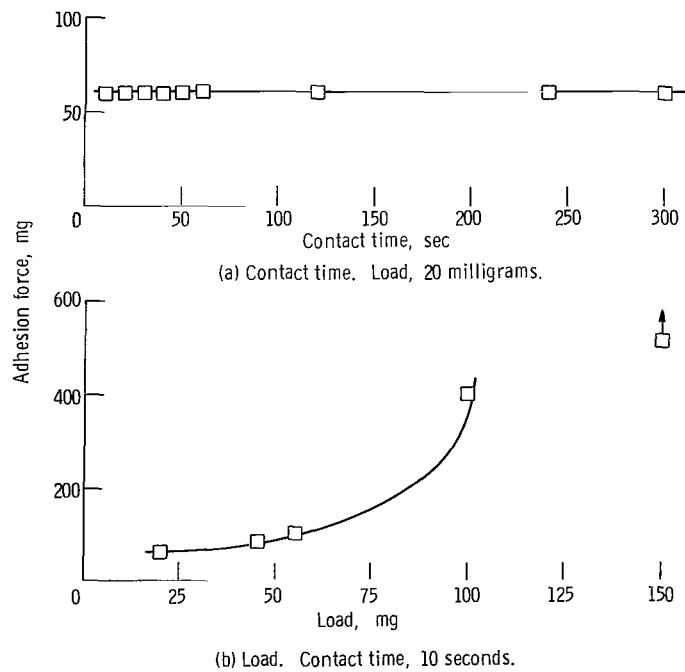


Figure 8. - Force of adhesion for tungsten in contact with nickel (111) surface as function of contact time and load. Tungsten diameter, 1.0 millimeter; fiber temperature, 20° C; ambient pressure, 8.0×10^{-11} torr.

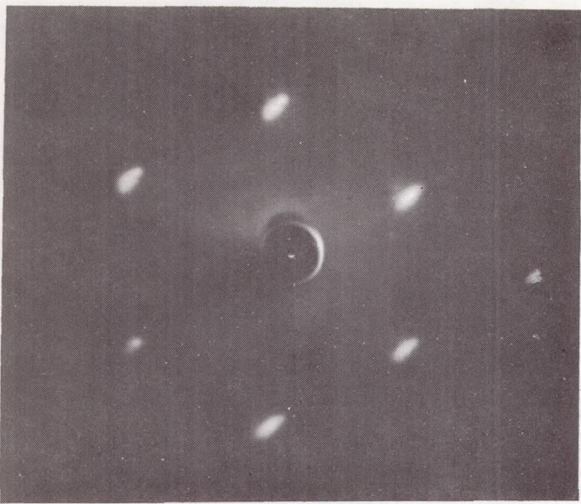
amined by LEED. Experiments were therefore conducted with a tungsten fiber contacting the nickel surface. The data of figure 8 present the adhesion force as a function of contact time at a fixed load of 20 milligrams and as a function of load for a fixed contact time of 10 seconds. In figure 8(a) the adhesion force is essentially independent of contact time.

The data of figure 8(a) are to be contrasted with those of figure 7(a) where microplastic (creep) of copper occurred. In figure 8(a) the material which will deform should be nickel. Nickel, however, is nearly twice as resistant to deformation as copper. Thus, under equivalent load conditions at the interface, nickel should behave less plastically than copper. The adhesion data of figure 8(a) indicate that it does. The nickel surface does, however, deform with residual material strain as shown by the LEED pattern of figure 9(a). The spots are no longer sharp as in figure 4(b) but have become elongated due to permanent lattice strain.

Figure 9(a) should be contrasted with figure 5(a) where lattice strain appears not to have occurred to any appreciable extent. The difference is due to two factors: (1) the copper of figure 5(a) is straining rather than the nickel in figure 9(a) and (2) the nickel-copper alloy formed in figure 5(a) would be more resistant to strain than the pure metal. Thus, while strain occurred to nickel under a 20-milligram load, it did not alter the adhesion force measured in figure 9(a). If a more sensitive device could have been used, some difference in adhesive force as a function of contact time should have been observed.

The data of figure 8(b) indicate the effect of load on adhesion. Figures 9(b), (c), (d), and (e) indicate the surface after adhesion at various loads as seen by LEED. The extent of surface deformation increased with increasing load. It should be noted in figure 8(b) that at 100 milligrams load, a marked increase in adhesion force has occurred. Careful examination of figure 9(e) shows that, in addition to surface streaking, spot splitting appears to have occurred. The pattern of figure 9(e) is believed to reflect localized twinning in the zone of contact which occurred during deformation. Normally, twinning in a crystal having a face-centered cubic structure results in an alteration of the packing arrangement from ABC ABC to CBA CBA. The first surface layer, or B layer, is the same in both the crystal and its twin. In the twin of figure 9(e), an A and C structure may exist on the surface (see fig. 3) with a common B subsurface layer.

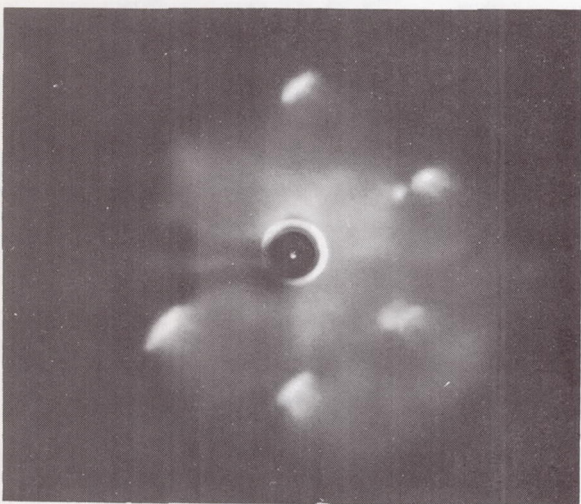
From the data presented thus far, it can be seen that the choice of mating surface has a pronounced effect on the behavior of a clean nickel surface. If the mating surface (copper) is less resistant to strain than the nickel, little, if any, change in nickel occurs. When the mating surface (tungsten) is more resistant to strain, marked strain will occur in nickel even at loads as low as 20 milligrams. A surface compound was observed to form with copper in contact with nickel. This occurred because both surfaces were clean. Experiments were conducted to determine the effect when one surface was not clean but contained an oxide. When nickel-copper experiments were conducted with oxidized cop-



(a) 20 milligrams; 75 volts.



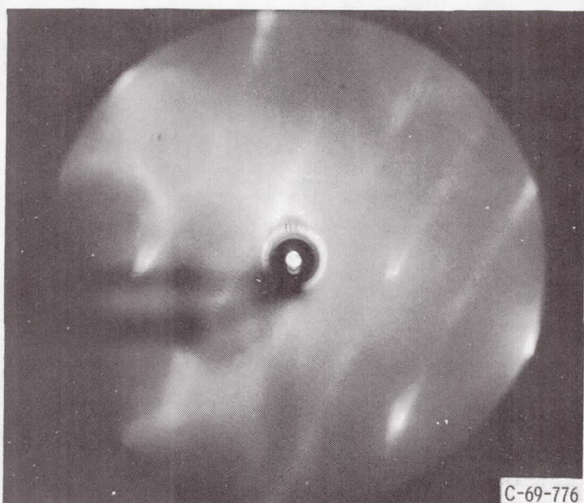
(b) 40 milligrams; 75 volts.



(c) 60 milligrams; 75 volts.



(d) 80 milligrams; 75 volts.



(e) 100 milligrams; 75 volts.

Figure 9. - Photographs of nickel (III) surface after contact by clean 1-millimeter-diameter tungsten fiber.

per, no intermetallic structure was observed to form. When experiments were conducted with oxidized tungsten, some interesting results were observed with LEED.

ADHESION WITH OXIDIZED TUNGSTEN

Experiments were made at various loads with a tungsten fiber which had been deliberately preoxidized contacting the nickel (111) surface. The LEED patterns obtained after adhesion experiments at various loads are presented in figure 10. At a load of 20 milligrams, oxygen was transferred from the oxidized tungsten tip to the nickel surface resulting in a chemisorbed layer of oxygen giving a Ni (111) $3\times3 - R(30^\circ)$ structure. This means that the oxygen has three times the lattice spacing in the [01] and [10] directions and is rotated with respect to its 30° . The structure is shown schematically in figure 11. Note in figure 10(a) that the amount of surface deformation is not as extensive as observed in figure 9(a) in the absence of oxygen. This is due to a reduction in adhesion in the presence of oxygen. The adhesion forces measured corresponding to figure 10 were markedly lower than those obtained in the absence of oxygen (fig. 8).

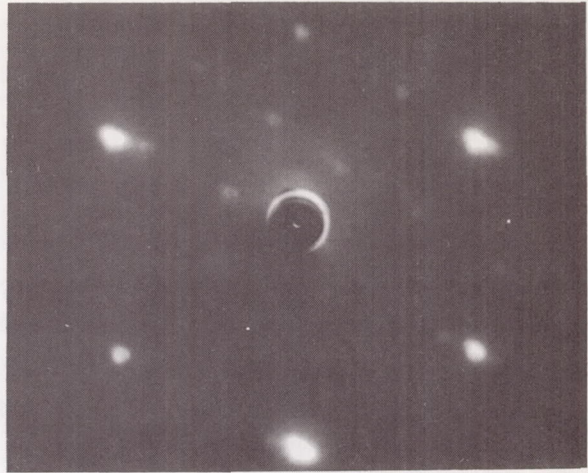
In figure 10, when the load reached 150 milligrams, the surface had undergone strain and both the nickel and the oxygen spots had become elongated. The interesting aspect of figures 10(a) to (e) is that oxygen is transferred from tungsten to nickel in an ordered fashion just as it might from the gas phase. This would seem to indicate fairly conclusively that oxygen rearrangement takes place on the surface after transfer.

Nickel will take up surface oxygen into its bulk (ref. 10). If then, the surface structure of figure 10(e) is in fact chemisorbed oxygen, simple heating should bring about oxygen diffusion into nickel. Heating the nickel surface of figure 10(e) to $1000^\circ C$ for 30 minutes resulted in the LEED pattern of figure 10(f) where the chemisorbed oxygen has been shown to dissolve completely in the nickel (ref. 10). The strain pattern of the nickel is, however, still prominent.

The LEED patterns of figure 10 indicate that oxygen from metal oxides may be transferred from one surface to another. Thus, reviewing briefly, with clean copper in contact with clean nickel, copper arranged itself in an orderly fashion on the nickel surface after the copper was pulled from its parent lattice sites by the adhesion process. With clean tungsten, transfer was observed from nickel to tungsten with strain in the nickel surface. With clean metals in contact, the cohesively weaker metal transfers to the stronger. The modulus of elasticity of a metal reflects the atomic cohesive strength and therefore the forces required to separate surfaces after adhesion (see relation in reference to copper-nickel).



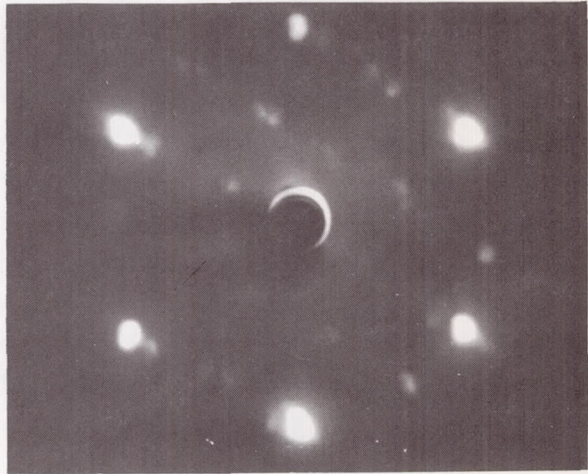
(a) 20 milligrams; 75 volts.



(b) 40 milligrams; 75 volts.



(c) 60 milligrams; 75 volts.



(d) 100 milligrams; 65 volts.



(e) 150 milligrams; 65 volts.



(f) 150 milligrams; 65 volts (after 30-minute anneal at 1000° C.).

C-69-777

Figure 10. - Photographs of nickel (111) surface after contact of that surface with 1-millimeter-diameter oxidized tungsten fiber at various loads.

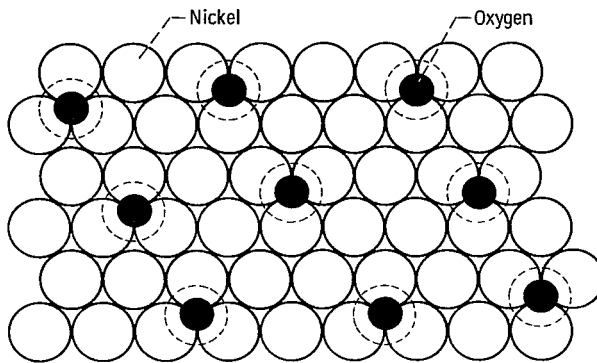


Figure 11. - Transfer of oxygen to (111) nickel surface from oxidized tungsten (see photograph of LEED pattern in fig. 10(a)).

With oxidized tungsten, the clean nickel reduces the tungsten oxide by oxygen transfer. The reduction probably results in the formation of a lower tungsten oxide:

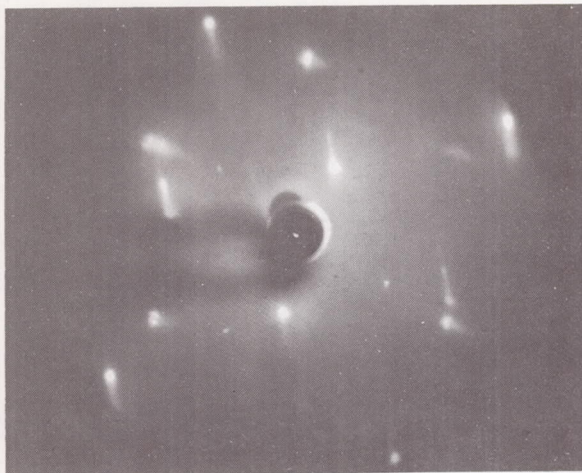


Examination of the chemical relations indicate a less stable oxide for nickel than for tungsten. The oxides of tungsten, however, would vary in their dissociation energies. The removal of single oxygens from WO_3 becomes successively more difficult with the removal of each oxygen. The removal of the first oxygen should be relatively easily achieved. The reduction, for example, of WO_3 to WO_2 with hydrogen may be achieved at a temperature of 750°C or less.

The presence of the oxide on tungsten resulted, in addition to oxygen transfer, in a reduction of nickel strain. This reduction in nickel strain under equivalent loads exists from two effects, both of which contribute to the change in strain. These are (1) the presence of the oxygen reduces the force of adhesion and (2) the transfer of oxygen to the nickel surface imparts to it greater resistance to strain (Roscoe Effect) (ref. 13). In relation to the first, as the amount of metal-to-metal contact is reduced, thereby reducing the adhesive force, less metal is strained in tension on surface separation. It should be noted that adhesion still occurs with these thin oxygen films present. It would be of interest to know if this reducing power of the clean nickel surface will effect oxygen transfer from a more stable oxide than tungsten oxide.

ADHESION WITH QUARTZ

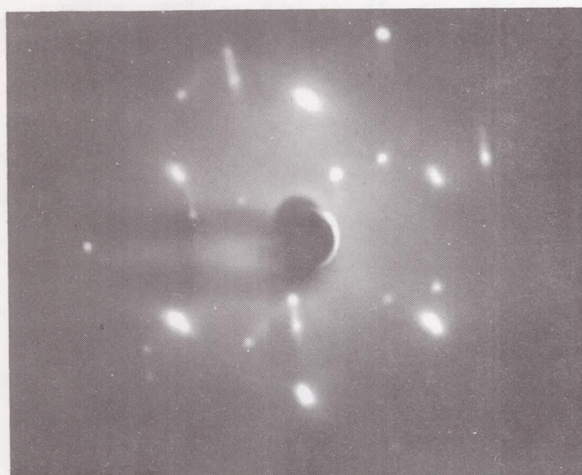
Oxygen is much more strongly bonded in silicon dioxide than in tungsten oxide. Adhesion experiments were therefore conducted with a quartz fiber contacting the nickel



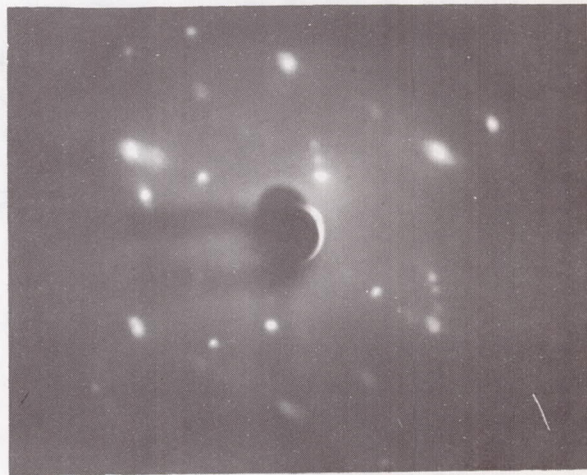
(a) 20 milligrams; 105 volts.



(b) Alongside 20 milligrams contact zone, 105 volts.



(c) 40 milligrams; 105 volts.



(d) 140 milligrams; 105 volts.



(e) 140 milligrams; 105 volts (after heating to 1000° C).

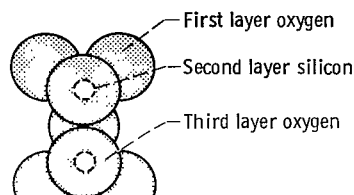
Figure 12. - Photographs of nickel (111) after contact of that surface with 1-millimeter-diameter quartz fiber.

(111) surface at various loads to determine the activity of a clean surface with respect to a very stable oxide. LEED patterns obtained are presented in figure 12. In figure 12(a) new streaked spots appear in the basic nickel pattern (contrast fig. 12(a) with pattern of fig. 4(b) for clean nickel).

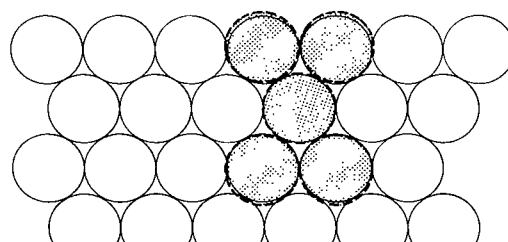
If a LEED pattern is taken alongside the actual adhesion contact zone, the pattern of figure 12(b) is obtained. It reflects the presence of something on the surface since intensity has been diminished. Figures 12(c) and (d), much like figure 12(a), indicate the presence of material transfer to the nickel surface. The question is whether the material transferred is oxygen or silicon dioxide.

If the transferred material in figures 12(a), (c), and (d) is simply oxygen, then heating to 1000° C should be sufficient to diffuse the oxygen into the nickel as was observed in figure 10(f) with oxidized tungsten. Heating, however, resulted not in the obtaining of a clean nickel surface, but rather the pattern of figure 12(e). This pattern should be contrasted with that of figure 10(a) where oxygen formed with the nickel a Ni (111) $3 \times 3 - R(30^{\circ})$ structure. Careful examination of figure 12(e) indicates three sets of spots. There are those of the basic nickel structure, with a second set of lesser intensity which form a distorted (2×2) structure and a third set of least intense spots whose pattern is not readily discernible. The pattern is not that simply of oxygen on the surface.

The atomic match of oxygen of silicon dioxide to the nickel (111) surface is shown in figure 13. The matching of a silicon dioxide dimer to the nickel surface results in a reasonable fit. It is this matching which may account for the transfer of silicon dioxide to



(a) Dimer of SiO_4 tetrahedron.



(b) Nickel (111) surface.

Figure 13. - Possible bonding sites for oxygen of silicon dioxide bonding to (111) nickel surface.

the nickel surface in figure 12(e) rather than oxygen as was observed with tungsten oxide.

A difficulty arises when the pattern of figure 12(e) is regarded as transferred silicon dioxide being present on the nickel surface. The silicon dioxide (if, in fact, that is what is present on the nickel surface) undergoes rearrangement on heating into an ordered structure. This was not observed with a rhenium (1010) surface in a similar study (ref. 20). The difference in results may be explained in terms of the amount of silicon dioxide transferred to the two different metals. With rhenium, the oxygen surface fit appeared to provide for bonding to alternate rows of rhenium atoms which, because of atomic mismatch, would produce considerable stress in the silicon dioxide. This stress produced subsurface fracture in the silicon dioxide. As a consequence, particles of silicon dioxide transferred to the rhenium surface and would not rearrange on heating.

In figure 13, however, a good surface match between oxygen and nickel is observed. This may result in a minimal stress and the transfer of a monolayer (or less than a monolayer) of silicon dioxide. Such minimal transfer was observed with copper where there was a good lattice matching of copper to nickel.

In this study, reference is frequently made to strain in the surface resulting after adhesion contact. One may ask how such is possible, particularly in light of the loads used and the previous discussion. It is important to note that the strain being referred to is strain in the outermost atomic layer of the nickel. It is strain in a layer of atoms which on one side are not bounded by like atoms but rather have a free surface exposed to vacuum. Thus, while the coordination number for nickel in the bulk is 12, on the (111) surface it is only 9. The resistance of these surface atoms to strain is therefore less. Some simple area assumptions indicated that the elastic limit of such a surface layer may be orders of magnitude less than that for atoms in the bulk. This is a caution against the use of bulk properties in trying to understand the surface behavior of materials in adhesion.

The presence of chemisorbed gases on the surface of nickel in this investigation and rhenium in an earlier one (ref. 20) seem to indicate that the resistance to strain of the outermost layer of metal atoms is increased with the presence of a surface film. This is difficult to measure quantitatively because the presence of the gas also inhibits adhesion.

CONCLUSIONS

Based on the adhesion measurements made in this investigation with a nickel (111) surface and observations of that surface after adhesion measurement with LEED, the following conclusions are drawn:

1. For clean metal surfaces in contact, fracture in tension occurred in the material of lower cohesive strength. With copper in contact with nickel, it occurred in copper and with tungsten in contact with nickel, it occurred in nickel.

2. With clean copper in contact with nickel (111), a surface alloy was formed in the adhesion experiments.

3. Transfer of oxygen from tungsten oxide on a tungsten fiber to the clean (111) surface occurred in adhesion experiments. The oxygen rearranged on the surface into an ordered structure. This oxygen transfer is believed to result from the reduction of a higher oxide of tungsten to a low oxide by the clean nickel surface.

4. With the adhesion of quartz to nickel, transfer to the nickel surface occurred. Based on the nature of the LEED pattern, it is believed that quartz, rather than simply oxygen, transferred to the nickel surface.

Lewis Research Center,

National Aeronautics and Space Administration,

Cleveland, Ohio, February 25, 1969,

129-03-13-09-22.

REFERENCES

1. Davisson, C.; and Germer, L. H.: Diffraction of Electrons by a Crystal of Nickel. *Phys. Rev.*, vol. 30, no. 6, Dec. 1927, pp. 705-740.
2. Farnsworth, H. E.; and Madden, H. H.: The Mechanism of Oxygen Chemisorption on Nickel. *Advances in Chemistry Series No. 33*, Am. Chem. Soc., 1961, p. 114.
3. Germer, L. H.; and Hartman, C. D.: Oxygen on Nickel. *J. Appl. Phys.*, vol. 31, no. 12, Dec. 1960, pp. 2085-2095.
4. Germer, L. H.; MacRae, A. U.; and Hartman, C. D.: (110) Nickel Surface. *J. Appl. Phys.*, vol. 32, no. 11, Nov. 1961, pp. 2432-2439.
5. Germer, L. H.; and MacRae, A. U.: Nitrogen on Nickel Surfaces. *J. Chem. Phys.*, vol. 36, no. 6, Mar. 15, 1962, pp. 1555-1556.
6. Germer, L. H.; and MacRae, A. U.: Adsorption of Hydrogen on a (110) Nickel Surface. *J. Chem. Phys.*, vol. 37, no. 7, Oct. 1, 1962, pp. 1382-1386.
7. MacRae, A. U.: The Epitaxial Growth of NiO on a (111) Nickel Surface. *Appl. Phys. Letters*, vol. 2, no. 4, Feb. 15, 1963, pp. 88-90.
8. Park, Robert L.; and Farnsworth, H. E.: The Interaction of O₂ with a Clean (111) Nickel Surface. *Appl. Phys. Letters*, vol. 3, no. 9, Nov. 1, 1963, pp. 167-168.
9. Park, R. L.; and Farnsworth, H. E.: The Structures of Clean Nickel Crystal Surfaces. *Surface Sci.*, vol. 2, 1964, pp. 527-533.

10. MacRae, A. U.: Adsorption of Oxygen on the (111), (100), and (110) Surfaces of Clean Nickel. *Surface Sci.*, vol. 1, no. 4, 1964, pp. 319-348.
11. Gwathmey, Allan T.; Leidheiser, Henry, Jr.; and Smith, G. Pedro: Influence of Crystal Plane and Surrounding Atmosphere on Chemical Activities of Single Crystals of Metals. NACA TN 1460, 1948.
12. Buckley, D. H.: The Influence of Crystal Structure, Orientation and Solubility on the Adhesion and Sliding of Various Metal Single Crystals in Vacuum (10^{-11} Torr). Adhesion or Cold Welding of Materials in Space Environments. Spec. Tech. Publ. No. 431, ASTM, 1967, pp. 248-271.
13. Germer, Lester H.: The Structure of Crystal Surfaces. *Sci. Amer.*, vol. 212, no. 3, Mar. 1965, pp. 32-41.
14. May, J. W.: Electron Diffraction and Surface Chemistry. *Ind. Eng. Chem.*, vol. 57, no. 7, July 1965, pp. 18-39.
15. Palmberg, P. W.; and Rhodin, T. N.: Auger Electron Spectroscopy of FCC Metal Surfaces. *J. Appl. Phys.*, vol. 39, no. 5, Apr. 1968, pp. 2425-2432.
16. Hansen, Max: Constitution of Binary Alloys. Second ed., McGraw-Hill Book Co., Inc., 1958, p. 601.
17. Elliott, R. P.: Constitution of Binary Alloys. Second ed., First Supplement, McGraw-Hill Book Co., Inc., 1965, p. 378.
18. Gilman, J. J.: The Strength of Ceramic Crystals. Mechanical Behavior of Crystal-line Solids. Monograph 59, National Bureau of Standards, Mar. 25, 1963.
19. Roscoe, R.: The Plastic Deformation of Cadmium Single Crystals. *Phil. Mag.*, vol. 21, 1936, pp. 399-406.
20. Buckley, Donald H.: LEED Studies of Adhesion to a Rhenium Surface. NASA TN E-4915, 1969.

NATIONAL AERONAUTICS AND SPACE ADMINISTRATION
WASHINGTON, D.C. 20546
OFFICIAL BUSINESS

POSTAGE AND FEES PAID
NATIONAL AERONAUTICS AND
SPACE ADMINISTRATION

FIRST CLASS MAIL

POSTMASTER: If Undeliverable (Section 158
Postal Manual) Do Not Return

"The aeronautical and space activities of the United States shall be conducted so as to contribute . . . to the expansion of human knowledge of phenomena in the atmosphere and space. The Administration shall provide for the widest practicable and appropriate dissemination of information concerning its activities and the results thereof."

—NATIONAL AERONAUTICS AND SPACE ACT OF 1958

NASA SCIENTIFIC AND TECHNICAL PUBLICATIONS

TECHNICAL REPORTS: Scientific and technical information considered important, complete, and a lasting contribution to existing knowledge.

TECHNICAL NOTES: Information less broad in scope but nevertheless of importance as a contribution to existing knowledge.

TECHNICAL MEMORANDUMS: Information receiving limited distribution because of preliminary data, security classification, or other reasons.

CONTRACTOR REPORTS: Scientific and technical information generated under a NASA contract or grant and considered an important contribution to existing knowledge.

TECHNICAL TRANSLATIONS: Information published in a foreign language considered to merit NASA distribution in English.

SPECIAL PUBLICATIONS: Information derived from or of value to NASA activities. Publications include conference proceedings, monographs, data compilations, handbooks, sourcebooks, and special bibliographies.

TECHNOLOGY UTILIZATION PUBLICATIONS: Information on technology used by NASA that may be of particular interest in commercial and other non-aerospace applications. Publications include Tech Briefs, Technology Utilization Reports and Notes, and Technology Surveys.

Details on the availability of these publications may be obtained from:

SCIENTIFIC AND TECHNICAL INFORMATION DIVISION
NATIONAL AERONAUTICS AND SPACE ADMINISTRATION
Washington, D.C. 20546